

Modeling & Simulations of The Lamp Heating-type Rapid Thermal Processor

M. HATTORI

The RTP (Rapid Thermal Processor) is a single-wafer thermal processing apparatus used in the semiconductor field featuring high temperature ramp rates and fast processing. In recent years, the use of materials and processes in research and development applications under processing conditions not originally anticipated is expanding. To meet these needs, we worked on modeling, simulation and experimental analysis of heating phenomena by halogen lamps, optical properties of materials and thermal balance inside the furnace. Through these efforts, we clarified the points for carrying out highly accurate thermal processing performance under a broader range of conditions. In this paper, we describe the modeling and simulation of RTP, and the verification of the actual device.

Key Words: RTP, lamp annealing, silicon wafer, heat treatment

1. Introduction

Thermal processors for semiconductors can be roughly classified into two groups of furnaces and RTP (Rapid Thermal Processor)¹⁾. Furnaces are used to perform uniform thermal processing for extended periods of time in a stable environment and for batch production. RTPs, also known as lamp annealing devices, are used for single wafers and offer high ramp rate heating and fast processing. In semiconductor manufacturing, to date, RTPs have been used for formation of an extremely thin thermal oxide film as well as annealing and metal silicide contact formation, etc. following ion implantation¹⁾, however RTPs are also often used for materials other than silicon and for process R&D. Particularly in recent years, there has been an increase in cases of using RTPs in applications other than those originally anticipated, namely, to keep several stages of temperatures for fixed periods of time such as the multi-stage heating method used for solar cell electrode firing, or to keep a high temperature for an extended period of time. As such, there is a greater need for RTPs tailored specifically to R&D applications which can be used with ease for a broad range of applications. As such, from the perspective of practical modeling useful for RTP device development, we performed verification and identification of physical constants, as well as analysis of heating mechanisms and radiation thermometer measurement characteristics, etc. and leveraged the obtained results in the development of “DTL-6”²⁾, a desktop RTP with a lamp output of 24kW and heating area of 150mm squares. This article will

focus on the silicon wafer, which is typical target of RTP heating, to discuss the RTP modeling and simulation conducted for this development, as well as an actual verification using DTL-6.

2. RTP Basic Structure

Figure 1 shows the basic structure of an RTP. Near-infrared light emitted by a halogen lamp (lamp) is used as the heat source. As the target of the heating, the silicon wafer is positioned inside a quartz process tube, and the light source and quartz tube are enclosed in aluminum housing which features water-cooling means. Wafer temperature is measured using a radiation thermometer through an optical filter positioned on the aperture of the quartz tube. Moreover, nitrogen gas is used inside the housing to cool the lamp surface and housing itself.

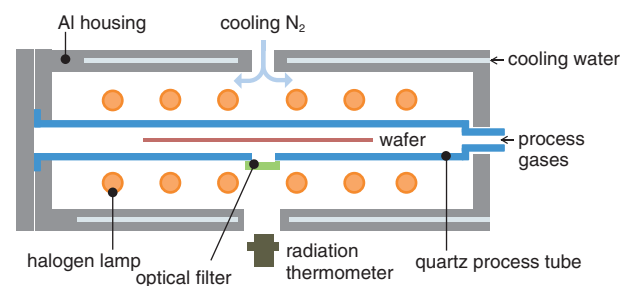


Fig. 1 RTP basic structure

3. Essential Summary of the Lamp Heating Process

3.1 Fundamental Equation for Silicon Wafer Heating

Figure 2 shows the heat balance during silicon wafer heating. It is thought that a silicon wafer with the temperature T_w emits a thermal energy of $\epsilon_w \sigma T_w^4$ and absorbs energy multiplied by its own emissivity to thermal energy radiated by the surrounding space. For heat balance, radiation is the domination therefore, here, first we must ignore convection and thermal conduction, and in order to generalize, we shall discuss using physical quantity per unit area.

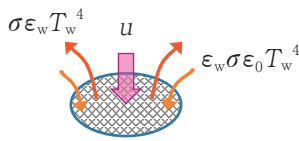


Fig. 2 Heat balance on a silicon wafer

Equation (1) shows the fundamental equation relating to wafer heating.

$$C_w \frac{dT_w}{dt} = u - \sigma (\epsilon_w T_w^4 - \epsilon_w \epsilon_0 T_0^4) \quad (1)$$

Where,

u : Effective irradiation energy density contributing to wafer heating [W/cm²]

C_w : Heat capacity per unit area of wafer [J/K]

T_w : Silicon wafer's temperature [K],

T_0 : Ambient temperature [K]

ϵ_w : Silicon wafer's emissivity,

ϵ_0 : Ambient emissivity

σ : Stefan-Boltzmann constant [= 5.68 × 10⁻¹²W/cm²]

Here, if we consider the point where the lamp illuminates in a thermal equilibrium state at room temperature ($T_w^4 = \epsilon_0 T_0^4$), then Equation (1) becomes

$$u = C_w \frac{dT_w}{dt} \quad (2)$$

and if the desired ramp rate is applied, it is possible to find the lamp energy density required for heating. If this value is made u_m then it is possible to obtain an approximate of the wafer's maximum attainable temperature, T_{wm} [K], from u_m .

In other words, if we establish $dT_w/dt = 0$ in Equation (1)

$$T_{wm} = \left[\frac{u_m}{\epsilon_w \sigma} + \epsilon_0 T_0^4 \right]^{1/4} \quad (3)$$

and if we ignore T_0^4 in relation to T_w^4 ,

$$T_{wm} \sim (u_m / \epsilon_w \sigma)^{1/4} \text{ [K]} \quad (4)$$

From Equations (2) and (4), for example, in order to heat a $\phi 150$ SEMI spec silicon wafer ($t = 0.675$ mm, $C_w = 0.114$ J/Kcm², $\epsilon = 0.67$) at 100°C/second, $u_m = 11.4$ W/cm² would be necessary and, at this time, $T_{wm} \sim 1315$ K (= 1042°C).

If a wafer for crystal silicon solar cells ($t = 0.2$ mm, $C_w = 0.034$ J/Kcm², $\epsilon = 0.9$) is heated with this energy, the ramp rate would be 335°C/second and the attainable temperature would be $T_{wm} \sim 1222$ K (= 949°C).

Actually, there is the component of ambient temperature T_0^4 , therefore the maximum attainable temperature would be higher than the value shown above.

In this way, the ramp rate and the maximum temperature which are basic specifications of device cannot be determined independently.

3.2 Optical Absorption/Radiation Temperature and Wavelength Dependency of a Silicon Wafer

It is well-known that the spectral emissivity of silicon wafers is highly dependent on temperature³⁾. Figure 3 shows the spectral emissivity of a silicon wafer. Silicon emissivity has high temperature dependency up to 600 °C in a wavelength region with an optical absorption edge of 1.1 μm or more. Emissivity is a parameter to be specified at temperature measurement using a radiation thermometer however, due to the fact that, for physical optical absorption, emissivity = absorptance, this temperature dependence must be considered when discussing the heating process of silicon wafers. Normally, this emissivity change would be found by calculating the area surrounded in curved lines corresponding to each temperature in Fig. 3, however as this temperature dependence is thought to be caused by electronic transition, we assumed it would adhere to Fermi-Dirac's distribution function and expressed it as Equation (5).

$$\epsilon(T) = \epsilon_1 + \frac{\epsilon_2 - \epsilon_1}{1 + \exp\left(\frac{T_2 - T}{B}\right)} \quad (5)$$

Where,

ϵ_1 : Initial emissivity at low temperature

ϵ_2 : Final emissivity

T_2 : Temperature where emissivity becomes ϵ_2

B : Parameter which adjusts the emissivity change temperature range

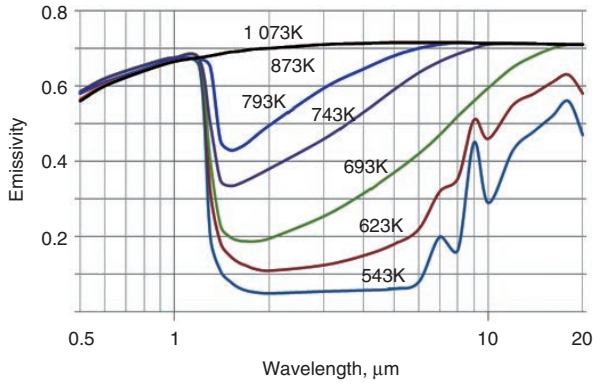


Fig. 3 Spectral emissivity of a silicon wafer

4. RTP Heat System Modeling

4. 1 Interaction of Heat within an RTP

Inside the RTP, the lamp heats not only the silicon wafer, but also the quartz tube and housing. Moreover, there is interaction between the heat of the wafer and quartz tube, and the quartz tube and housing, respectively. Figure 4 shows the heat radiation of each part.

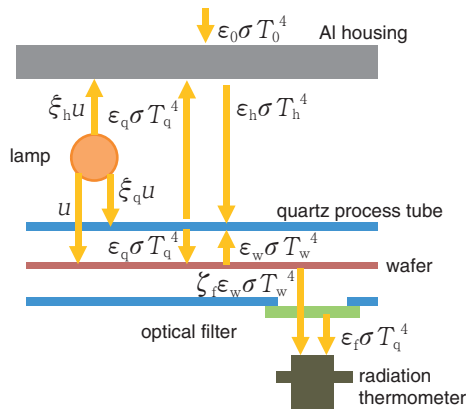


Fig. 4 Interaction of heat radiation within the RTP

If this is established as a state equation, it would express as Equation (6).

$$\frac{d}{dt} \begin{bmatrix} T_w \\ T_q \\ T_h \end{bmatrix} = \sigma \begin{bmatrix} -\frac{\epsilon_w}{C_w} & \frac{\epsilon_w \epsilon_q}{C_w} & 0 \\ \frac{\epsilon_q \epsilon_w}{C_q} & -\frac{\epsilon_q}{C_q} & \frac{\epsilon_q \epsilon_h}{C_q} \\ 0 & \frac{\epsilon_h \epsilon_q}{C_h} & -\frac{\epsilon_h}{C_h} \end{bmatrix} \begin{bmatrix} T_w^4 \\ T_q^4 \\ T_h^4 \end{bmatrix} + \begin{bmatrix} \frac{1}{C_w} \\ \xi_q \frac{1}{C_q} \\ \xi_h \frac{1}{C_h} \end{bmatrix} u + \begin{bmatrix} 0 \\ 0 \\ \frac{\epsilon_h \sigma \epsilon_0 T_0^4}{C_h} \end{bmatrix} \quad (6)$$

Where,

T_q, T_h : quartz tube, housing temperature [K]

C_q, C_h : quartz tube, heat capacity per housing unit area [J/K]

ϵ_q, ϵ_h : quartz tube, housing emissivity

ξ_q, ξ_h : Effective irradiation energy ratio toward quartz tube/housing in relation to wafer effective irradiation energy

The silicon wafer, quartz tube and housing each have different spectroscopic absorption properties therefore, technically speaking, there is a need to find the energy contributing to the heating of each from the lamp's emitting state, and we simplified a model expressing this as the ratios ξ_q and ξ_h in relation to the input to the silicon wafer, u .

4. 2 Temperature Detected by a Radiation Thermometer

By converting the temperature into radiation energy, add and subtract calculations become possible. Because the thermal radiation ray from the housing does not incident as a direct ray on the radiation thermometer, it is the radiation ray from the wafer and the radiation ray from the observation window on the quartz tube that are detected by the radiation thermometer. Therefore, as the output of Equation (6), the radiation energy E_{rad} detected by the radiation thermometer is expressed by Equation (7), and observation temperature T_{rad} is given by Equation (8).

Where, we have made filter temperature = quartz tube temperature.

$$E_{rad} = \sigma \begin{bmatrix} \zeta_f \epsilon_w \eta_{rad}(T_w) & \epsilon_f \eta_{rad}(T_q) & 0 \end{bmatrix} \begin{bmatrix} T_w^4 \\ T_q^4 \\ T_h^4 \end{bmatrix} \quad (7)$$

Where,

ζ_f : optical filter's transmission,

ϵ_f : optical filter's emissivity

$\eta_{rad}(T)$: the radiation energy ratio of the wavelength region detected by the radiation thermometer at temperature T

$$T_{rad} = \left(\frac{E_{rad}}{\epsilon_w} \right)^{1/4} \quad (8)$$

4. 3 Temperature Dependence of the Physical Constant

In modeling to date, we have treated physical quantities like a constant, however in reality, temperature dependence must be considered, therefore we expressed them by polynomial approximation to make them easy to use for calculations. For the specific heat of quartz, we scanned a graph⁴⁾ used in technical documentation prepared by the manufacturer and carried out quartic approximation (this is not the C_q of Equation (6) which

Table 1 Polynomial approximation coefficient of temperature dependent parameter

	a_5	a_4	a_3	a_2	a_1	a_0
$c_q(\tilde{T})$		-8.45×10^{-1}	3.53	-5.59	4.18	-7.52×10^{-2}
$\eta_{rad}(\tilde{T})$	2.46	-1.20×10	2.23×10	-1.95×10	7.32	-5.90

establishes $c_q(T)$ [J/gK] but rather the specific heat of quartz as a material).

η_{rad} is Planck’s radiation law

$$L(\lambda, T) = \frac{2\pi hc^2}{\lambda^5} \frac{1}{\exp\left(\frac{hc}{k\lambda T}\right) - 1} \quad (9)$$

Where, we used

k : Boltzmann constant [1.381×10^{-23} J/K],

h : Planck constant [6.626×10^{-34} J s],

c : Light speed [2.998×10^8 m/s]

and performed polynomial approximation by calculating the wavelength region $\lambda_1 \leq \lambda \leq \lambda_2$ radiation energy and all radiation energy ratio when the temperature is T [K].

$$\eta_{rad}(T) = \frac{\int_{\lambda_1}^{\lambda_2} L(\lambda, T) d\lambda}{\int_0^{\infty} L(\lambda, T) d\lambda} \quad (10)$$

Table 1 shows the polynomial approximated coefficients of $c_q(\tilde{T})$ and $\eta_{rad}(\tilde{T})$. Where, $\tilde{T} = T/1000$ and a_i are coefficients of \tilde{T}^i when the polynomial expression is expressed as $\sum_{i=0}^n a_i \tilde{T}^i$, therefore ξ_q and ξ_h . Are quantities introduced as the references to express heating energy on the silicon wafer, which is an observable quantity regarding the extent to which the energy emitted by the lamp is supplied to the quartz tube and housing. This parameter value was found based on experiments and analysis of halogen lamp which were executed separately.

For ξ_h , the optical absorption region is biased toward the short wavelength side of the spectrum emitted by the lamp therefore, we estimated 0.05 to 0.1 with consideration to the emissivity of the aluminum semi-gloss surface at a wavelength of 1 μm . Housing has a heat capacity 20 times greater than the other portions, good thermal conduction and is water-cooled, therefore is practically not affected at all if ξ_h changes.

Quartz will transmit rays with a cut-off wavelength of 4.5 μm or less and absorb rays with wavelengths over this⁵⁾. A halogen lamp is of a structure whereby a tungsten filament is enclosed in a quartz tube (bulb), and rays equivalent to or greater than the cut-off wavelength are not emitted but the bulb surface⁶⁾ absorbs filament rays until it increases in temperature between 250 and 800 $^\circ\text{C}$ then the heat radiation from the bulb (secondary ray) heats the quartz tube. The ξ_q exceeds 0.4 at the minimal output of u , however decreases to 0.05 at maximum lamp output, therefore we performed linear interpolation between these two.

5. Model Verification

5.1 Silicon Wafer Temperature Increase Process

Figure 5 shows the result of using the DTL-6 to apply full power to the lamp (24kW) and heat, as well as the result of a simulation considering the fluctuation in emissivity in accordance with Equation (4). (1) is a $\phi 150$ SEMI spec silicon wafer and (2) is a polycrystalline silicon bare wafer for solar cells (it must be noted that

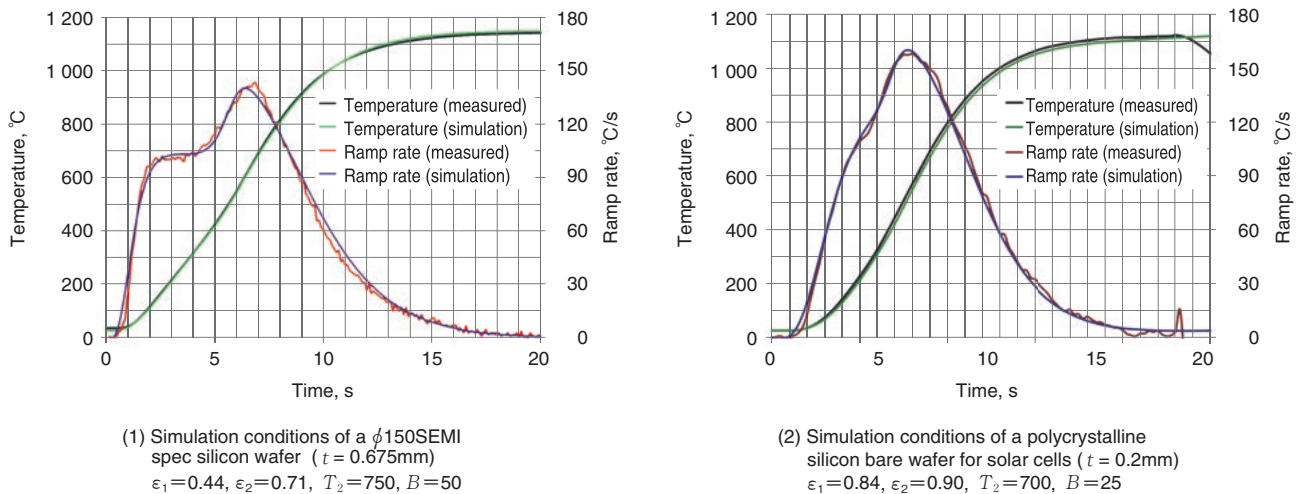


Fig. 5 Comparison of measured and simulated wafer temperature-increase profile and ramp rate

the time axis and ramp rate scales differ for both).

The thermocouple generates heat due to the lamp light and a large measurement error occurs therefore⁷⁾, temperature measurement was performed using measurement wafer which was embedded thermocouple tip and fixed with ceramic bond (TC wafer). The ramp rate was calculated from the temperature profile. Furthermore, for the simulation, we used the open source numerical calculation software, Scilab.

The ramp rate of a SEMI wafer stagnates at around 100 to 400°C, and due to the fact that this phenomenon was reproduced in a simulation also, depending on the temperature dependence of emissivity, if one wished to perform more accurate processing in this temperature range, it is clear that caution is needed. Meanwhile, in the case of solar cell wafers, which have an anti-reflective layer on the surface in order to absorb as much light as possible, emissivity change is minimal, therefore the impact of the abovementioned phenomenon is slight.

5. 2 Effect of Disturbance

When temperature control is performed to keep a high temperature for a set period of time using radiation thermometer, a phenomenon occurs in which the actual temperature of the wafer decreases although the control temperature is constant. This state is shown in Fig. 6 (1). The control temp. shown in the figure is the instruction value of the radiation thermometer used in feedback control, the wafer temp. is the instruction value of the TC wafer and the MV (manipulate value) is the lamp’s power control value. This kind of phenomenon was raised as a problem when RTPs began being used for processing requiring high temperature to be kept for a certain period of time. For this phenomenon, we carried out the simulation of temperature control with T_{rad} feedback using the models of Equation (6) though (8). Figure 6 (2) shows the results of this simulation. T_{rad} is a value of Equation (8), and equates to the measured control

temp. T_w is the measured wafer temp. of component 1, Equation (7).

Conventionally, in order to deal with this phenomenon, processing would be once performed using a TC wafer, and the processing recipe (processing pattern given to the device as a command value) was corrected by measuring the temperature decrease. With such simulation, it was possible to predict the compensation value.

6. Conclusion

As described above, we performed modeling to verify factors such as the optical absorption of a silicon wafer, the interaction of heat inside an RTP, radiation ray input into a radiation thermometer and the temperature dependencies of materials and physical quantity. We also performed simulations applying the RTP to a “wider usage scope and more rigorous thermal processing.” We performed some extremely rough simplifications and approximations for portions, however these can be said to have reproduced the actual phenomena with good accuracy. These analysis results clarified the necessary and sufficient conditions for realizing physical specifications in the development of the desktop RTP, DTL-6, and directly led to the achievement of a device with higher efficiency, reduced size and lower cost. As for the non-physical aspect, these analysis results were utilized for the implementation of various functions compensating process experimentation, such as the emissivity interpolation functionality preventing the phenomenon described in Section 5.

This article only introduced the application of RTP in silicon wafer processing, however RTPs can be used for many materials and we intend to offer the knowledge and know-how obtained here for our customers in their development of new materials and processes.

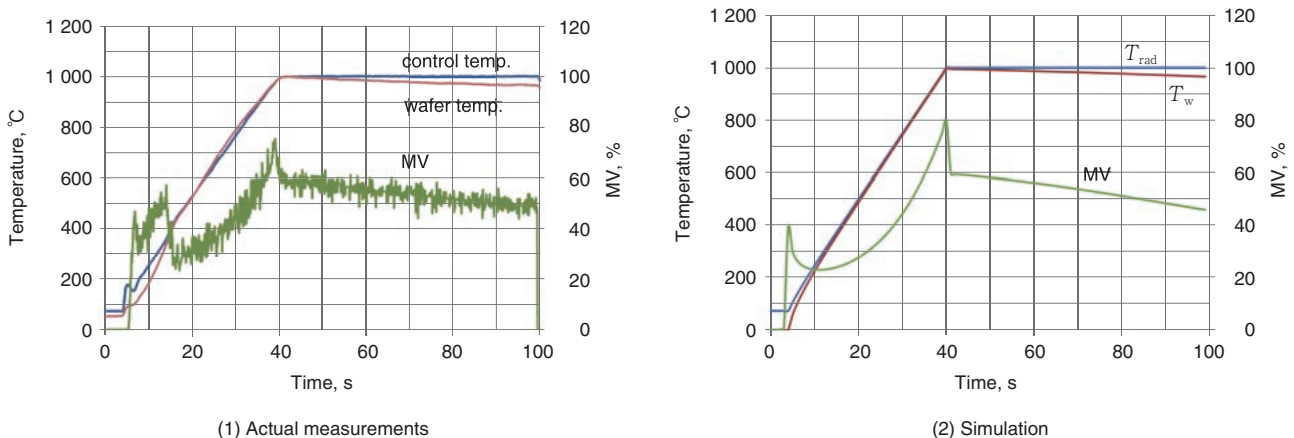


Fig. 6 Wafer actual temperature error caused by temperature control using radiation thermometer feedback

7. Acknowledgment

The modeling and simulations featured in this article were accomplished in a course called Fundamental PIER Program⁸⁾ (Pioneering Integrated Engineering Research Program), which is being implemented at the Department of Adaptive Machine Systems Graduate School of Engineering, Osaka University, where the author serves as a visiting lecturer. Fundamental PIER Program is an industry-academia partnerships course for practicing actual R&D whereby a corporate coach introduces a development issue for students to solve over a period of one year. I would like to extend thanks to the students who participated in the Koyo Thermo Systems team from FY2013 to FY2016 and undertook the tasks of investigating literature and various data, as well as conducting experiments and analyses. I wish these students great success moving forward. Moreover, I would like to prepare another article to announce the modeling and simulations of the halogen lamp, as well as the measurement characteristics of the wavelength region detected by the radiation thermometer; all of which was omitted in this article.

References

- 1) K. MAEDA: Hajimete no handoutai-seizousouchi, Kogyo Chosakai Publishing Co., Ltd(1999)118-127 (in Japanese).
- 2) http://www.koyo-thermos.co.jp/products/handou/handou_dtl6.html
- 3) N. M. RAVINDRA, B. SOPORI, O. H. GOKCE, S. X. CHENG, A. SHENOY, L. JIN, S. ABEDRABBO, W. CHEN, and Y. ZHANG: 「Emissivity Measurement and Modeling of Silicon-Related Materials: An Overview」, International Journal of Thermophysics, Vol. 22, No. 5, September 2001(2001).
- 4) 「Sekieigarasu gijutugaido1-sekieigarasu no kagakuteki, buturiteki tokusei」, Shin-Etsu Quartz Product Co., Ltd (2010)9 (in Japanese).
- 5) 「Sekieigarasu gijutugaido2-sekieigarasu no kougakuteki tokusei」, Shin-Etsu Quartz Product Co., Ltd (2010)3 (in Japanese).
- 6) 「Halogen lamp no kiso」, Light Edge, No. 22 USHIO INC., (2001) (in Japanese).
- 7) M. HATTORI: 「Lamp kanetu-souti niyoru Si-wafer no netusyori」, Jisedai no taiyou-dennchi · taiyoukouhatsuden - sono hatudennkouritsu koujou, youto to sijou no kanousei, TECHNICAL INFORMATION INSTITUTE CO., LTD(2018)423-428 (in Japanese).
- 8) <http://www.ams.eng.osaka-u.ac.jp/fpp-j.html>



M. HATTORI*

* Product Development Dept., Koyo Thermo Systems Co., Ltd.